


Variation in the post-smolt growth pattern of wild one sea-winter salmon (*Salmo salar* L.), and its linkage to surface warming in the eastern North Atlantic Ocean

Christopher D. Todd¹  | Nora N. Hanson² | Lars Boehme¹ | Crawford W. Revie^{3,4} | Ana R. Marques^{3,5}

¹Scottish Oceans Institute, School of Biology, University of St Andrews, St Andrews, UK

²Marine Scotland Science, Salmon and Freshwater Fisheries Laboratory, Pitlochry, UK

³Department of Health Management, Atlantic Veterinary College, University of Prince Edward Island, Charlottetown, Prince Edward Island, Canada

⁴Department of Computer and Information Sciences, University of Strathclyde, Glasgow, UK

⁵Research Group for Genomic Epidemiology, National Food Institute, Technical University of Denmark, Kgs. Lyngby, Denmark

Correspondence

Christopher D. Todd, Scottish Oceans Institute, School of Biology, University of St Andrews, St Andrews, Fife, Scotland KY16 8LB, UK.
Email: cdt@st-andrews.ac.uk

Funding information

CERC Aquatic Epidemiology Visiting Scientist initiative at University of Prince Edward Island; Canada Excellence Research Chair in Aquatic Epidemiology

Abstract

Variation in circulus spacing on the scales of wild Atlantic salmon is indicative of changes in body length growth rate. We analyzed scale circulus spacing during the post-smolt growth period for adult one sea-winter salmon ($n = 1947$) returning to Scotland over the period 1993–2011. The growth pattern of the scales was subjectively and visually categorized according to the occurrence and zonal sequence of three intercirculus spacing criteria (“Slow”, “Fast” and “Check” zones). We applied hierarchical time-series cluster analysis to the empirical circulus spacing data, followed by *post hoc* analysis of significant changes in growth patterns within the 20 identified clusters. Temporal changes in growth pattern frequencies showed significant correlation with sea surface temperature anomalies during the early months of the post-smolt growth season and throughout the Norwegian Sea. Since the turn of the millennium, we observed (a) a marked decrease in the occurrence of continuous Fast growth; (b) increased frequencies of fish showing an extended period of initially Slow growth; and (c) the occurrence of obvious growth Checks or hiatuses. These changes in post-smolt growth pattern were manifest also in decreases in the mean body length attained by the ocean midwinter, as sea surface temperatures have risen.

KEYWORDS

cluster analysis, growth pattern, post-smolt, *Salmo salar*, scale circulus, SST anomaly

1 | INTRODUCTION

Counts and measurements of the numbers and spacing of growth rings (circuli) deposited on the calcified portion of teleost scales can provide detailed archival data on the age and growth history of individual fish (e.g., Bilton & Robins, 1971; Casselman, 1987; Fisher & Pearcy, 1990). With specific respect to Pacific and Atlantic salmonids, scale analyses have, over many decades, comprised the basis of growth assessments and the differentiation of stocks, age categories

and maturity groupings (e.g., DeVries & Frie, 1996; Fisher & Pearcy, 2005; Friedland & Haas, 1996; Fukuwaka & Kaeriyama, 1997; Jensen *et al.*, 2012; Reddin & Friedland, 1999; Shearer, 1992; Tattam *et al.*, 2003). The marine circuli on wild Pacific and Atlantic salmonid scales typically show considerable variation in their spacing, often in distinct zones of differing width which may reflect marked intra-seasonal variation in growth rate. A wider intercirculus spacing can be indicative of increased growth rate in body length (Fisher & Pearcy, 1990, 2005; Peyronnet *et al.*, 2015), but the latter may be manifest

This is an open access article under the terms of the Creative Commons Attribution License, which permits use, distribution and reproduction in any medium, provided the original work is properly cited.

© 2020 The Authors. *Journal of Fish Biology* published by John Wiley & Sons Ltd on behalf of Fisheries Society of the British Isles.

also by increased numbers of circuli (Haraldstad *et al.*, 2016). Thus, for example, from scale circulus measurements for Atlantic salmon smolts reared experimentally for 12 weeks, and at a range of temperatures and dietary regimes, Thomas *et al.* (2019) noted the rate of circulus deposition to increase with temperature. Circulus spacings did, however, show a complex interaction both with diet and temperature, and were widest at 10.5°C, narrower at 15°C and intermediate at 6°C. The narrow spacings at 15°C arose as a result of the rate of circulus deposition being disproportionately high in relation to individual growth rate in body length. Notwithstanding the likely complexity of environmental temperature and prey availability influencing circulus formation, measures of both the numbers and spacing of marine circuli for wild juvenile Atlantic salmon (*Salmo salar* L.) in their first (= post-smolt) marine growth season have been interpreted as indicators of growth variation, with possible linkage to changes in size-related mortality at sea (e.g., Friedland *et al.*, 2000, 2006, 2009; Hogan & Friedland, 2010; McCarthy *et al.*, 2008; Peyronnet *et al.*, 2015).

Following river emigration of a smolt, the typical pattern of marine growth of wild Atlantic salmon during the post-smolt growth season is for intercirculus spacing generally to increase up to a so-called First Summer Maximum (FSM; Friedland *et al.*, 1993; Peyronnet *et al.*, 2015) followed by a progressive decline to a series of tightly spaced circuli comprising a visually obvious winter annulus. The number of annuli permits the determination of the sea age of the individual adult fish at migratory return to freshwater. Whilst the deposition of a single annulus per calendar year is typical of salmon and many teleost species, it is notable that the scales of some tropical or subtropical fish species show two annuli per year. For example, the cyprinid *Labeo cylindricus* in Mozambique shows two growth checks per year – in April and in October – which are coincident with the conclusion of annual spawning and the occurrence of the physiological winter (Weyl & Booth, 1999).

Within the context of a typical pattern of once-yearly deposition of annuli – or “checks” of tightly spaced circuli – on teleost scales, it is recognized also that “false checks” (*sensu* Ottaway & Simkiss, 1977) can form on the scale during the active growth season. For species reared in aquaculture, changes in husbandry regime (e.g., movement of fish between ponds or switches in dietary feed) can result in the formation of a series of tightly spaced circuli similar to an annulus (e.g., Ibañez *et al.*, 2008). Bilton and Ricker (1965) first reported the occurrence of false checks on the scales of wild Pacific pink (*Oncorhynchus gorbuscha*) and chum (*O. keta*) salmon of known age. With respect to Atlantic salmon, the incidence of false checks on the scales of wild adults returning to freshwater across a range of years has been explicitly reported only by MacLean *et al.* (2000). Dating back to 1963, Marine Scotland Science have compiled detailed monitoring data and scale sample archives for multiple river stocks of Atlantic salmon returning to Scotland. From these, MacLean *et al.* (2000) found that whilst the occurrence of false checks during the first (post-smolt) growth season was sporadic up until the 1990s, their incidence in the late 1990s showed a significant increase. Those observations, coupled with previous studies linking variation in post-

smolt growth to long-term changes in year-class survival (e.g., Friedland *et al.*, 2000, 2009; Peyronnet *et al.*, 2015), highlight the potential importance to salmon stock management of a more detailed appraisal of marine growth variation (manifest as observable overall growth patterns or variation in zones of inter-circulus spacing) at the level of the individual fish. Here, we focus on variation in growth pattern based on circulus counts and spacings comprising the post-smolt growth season for time-series samples (1993–2011; Marine Scotland Science) of wild one sea-winter (1SW) Atlantic salmon returning to the River North Esk (East Scotland; 56°46'N, 02°26'W).

Discriminant function analysis (DFA) methods have been applied to scale circulus pattern measurements for individual fish in distinguishing wild and cultured steelhead trout (*Oncorhynchus mykiss*; Tattam *et al.*, 2003), and in roach (*Rutilus rutilus*; Britton, 2010). For Pacific and Atlantic salmonids, DFA has aided in the allocation of individuals to particular stocks and also the continent of origin for fish taken in mixed-stock fisheries (reviewed by Reddin & Friedland, 1999). In contrast to DFA, we here apply a hierarchical time-series clustering methodology to measures of variation in post-smolt marine circulus spacings up to the ocean winter annulus, with a view to objectively assessing the validity of subjectively and visually identified pattern categorizations for individuals. The fundamental difference between hierarchical time-series clustering and DFA lies in the latter relying upon previous knowledge of groups (i.e., “pattern”) and group memberships, and on the overall approach to shape-based classification. The exploratory hierarchical clustering approach applied here considers the shape of the entire time-series sequence in assigning cluster membership, whereas the discriminant analysis classifier would account for scale characteristics expressed through different predictor variables. We show that hierarchical time-series clustering has the potential for interpretable pattern discovery in Atlantic salmon populations.

2 | MATERIALS AND METHODS

2.1 | Scale samples and circulus data

The present data pertain to return-migrant 1SW adult salmon captured in commercial nets in the estuarine reach of the River North Esk between 1993 and 2011. Marine Scotland Science personnel monitored catches throughout the netting season, which terminated on 31 August in each year. Monitoring of catches was at least weekly and all fish captured on a given day were measured. The present data are for stratified subsamples ($n = 1947$; 96–114 fish per year) spanning the full available date range of 1SW return migrants captured within each year (typically April/May to end August). Fish were measured (fork length, rounded down to 0.5 cm) and weighed (to 0.01 kg), and scale samples removed from the standard region (Hanson *et al.*, 2019; Shearer, 1992). Scales were air-dried in paper packets and stored for further analysis. Scales were pressed on acetate strips and a single impression was photographed with a Leitz Wild M8

microscope; image analysis of circulus spacings was undertaken using AnalySIS software (Soft-Imaging Software GmbH; Münster, Germany). Images were calibrated with on-screen accuracy ranging from 3.16 to 6.57 μm per pixel, according to scale radius. For each image the single ocean winter annulus – comprising the typical series of tightly spaced and slightly thickened circuli – was identified, and all marine growth circuli from river emigration of the juvenile smolt to the conclusion of the ocean winter annulus were enumerated and measured. The winter annulus amongst the present samples comprised a median of four circuli (IQR 3–5; range 2–11 circuli). An estimate of the body length of each fish at the midpoint of the winter annulus was derived by back-calculation of scale measures, and by applying the correction factor of Hanson *et al.* (2019) to the estimate of body length of the smolt at river emigration. Growth in body length between smolt emigration and capture of the measured adult fish was assumed to be isometric with the scale radius.

The primary objective of the present study was an analysis of variability and heterogeneity of the pattern of individual growth during the first (post-smolt) growth season at sea, as indicated by variation in the spacings of the pre-annulus circuli. Accordingly, a subjective assessment was made for each scale whereby the overall growth pattern of post-smolt intercirculus spacing was visually classified according to the zonal incidence of three criteria (“Fast”, “Slow” and “Check” sequences). A sequence of widely spaced circuli was classified as “Fast” (F), more closely-spaced circuli as “Slow” (S), and circuli that were thickened and spaced similarly tightly to those of the subsequent winter annulus were allocated as a “Check” (C). Example scales showing the presently recognized SF, SFCF and F growth patterns are illustrated in Figure 1a–c, respectively, of Todd *et al.* (2014). Our recognition of a post-smolt growth Check is in accordance with the identification of “false checks” as reported by Ottaway and Simkiss (1977).

Here, when visually attributing a post-smolt (pre-winter) growth pattern (*e.g.*, SFCF) for individual fish, the Check grouping was allocated only if there were three or more contiguous circuli comprising the feature. In some instances, single or double spacings of “Fast” or “Slow” circuli separating distinct zones were recognized. For example, for a scale showing a continuous series of widely spaced circuli, followed by a late Check – which itself was separated from the winter annulus by a single wide intercirculus space – that fish was classified as FC. One especial challenge for some individual fish was the differentiation of the winter annulus circuli from a series of Check circuli that immediately preceded the start of the annulus (*e.g.*, fish that were visually allocated a pattern of SFC). Here, we adopted the same protocol as Todd *et al.* (2014) and Haraldstad *et al.* (2016) in distinguishing the annulus circuli according to their showing “cutback” in the scale region located at approximately 45° to the longest radius of the scale: two examples are illustrated by Todd *et al.* (2014; their Figure 1a,b). A secondary focus of the objective hierarchical time-series clustering analyses was to determine if the subjective, visual, classification of the growth pattern is supportable. Such would be indicated by a clear interpretable pattern structure among and between clusters, and perhaps also along the 19-year time-series.

The circuli analyzed and categorized for each fish included only those from river emigration of the smolt up to the commencement of

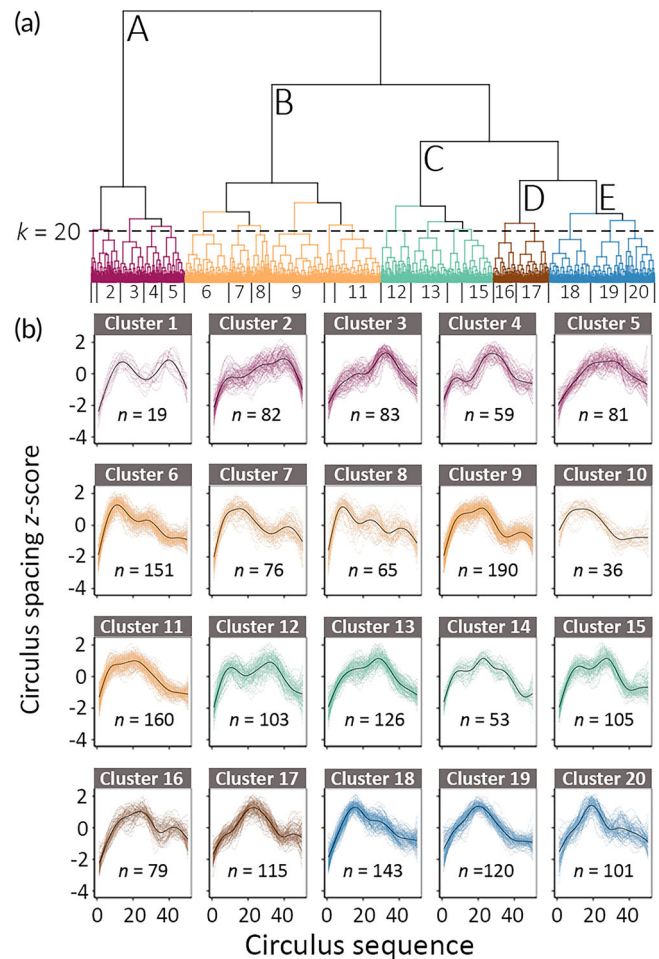


FIGURE 1 Hierarchical cluster analysis of intercirculus spacing for scales of *Salmo salar*. (a) The dendrogram for $k = 20$ using Euclidean distance and Ward linkage for z-scored and interpolated data. The five major sub-branches (A–E) and the 20 clusters are ordered sequentially from the left. (b) The standardized intercirculus spacing plots for the 20 clusters. Clusters are colour-coded and ordered as in (a). The LOESS fits for each cluster are shown as a black line and the number of fish per cluster (n) is also shown

the winter annulus. Given that the attribution of a Check sequence during the marine post-smolt growth period was visually influenced by the spacing of the winter annulus circuli for a given fish, it is important to note that there is among-fish variability in the spacing of the circuli comprising the annulus. The median spacing of the winter annulus circuli was 39.3 μm (IQR 35.6–43.2 μm), but this ranged between 22.4 and 71.9 μm for individual fish. For the present purposes, therefore, and prior to the cluster analyses, the spacings of the circuli comprising the post-smolt growth season for each fish were transformed by dividing by the mean spacing of the winter annulus circuli for that fish.

Because we here chose to analyze only the first (post-smolt) growth season at sea, the data comprise a varying number of intercirculus spacings for individual fish. To overcome this variation, the circulus data for each individual were linearly interpolated to achieve equal sequences of 50 spacings; this was the value for the individual

showing the largest number of pre-annulus circuli. This standardization permitted the application of different clustering parameters, with the assurance from previous studies (Ratanamahatana & Keogh, 2004) of unaltered accuracy under reinterpolation, for the longest, shortest or mean length of clustered time-series. In order to achieve clusters based on similar shapes, a z-score normalization also was performed on each sequence – followed, as part of the process, by a locally estimated scatterplot smoothing (LOESS) ($\alpha = 0.38$) – to highlight the underlying trend of each sequence without over-smoothing (Sardá-Espinosa, 2017).

2.1.1 | Hierarchical clustering

In applying time-series clustering, we explored several parameter settings for hierarchical clustering; all statistical analysis was undertaken using the computing environment R and the *dtwclust* package (R Core Team, 2018; Sardá-Espinosa, 2017, 2018). We undertook agglomerative hierarchical clustering, whereby every sequence starts as its own individual cluster and is sequentially grouped at each step of the algorithm according to the between-cluster and inter-group similarity (Hastie *et al.*, 2009). Inter-group dissimilarity is known also as linkage and, as for other parameters, the appropriate linkage method is unknown *a priori*. As such, four linkage methods were explored: Simple, Average, Complete and Ward's.

For the analysis of the z-scored data, we utilized the two most frequently applied distance functions in other domains: dynamic time warping (DTW) and Euclidean distance (Silva *et al.*, 2018). Euclidean distance often is used when measuring similarity in time-series clustering (Keogh & Kasetty, 2003). Clustering with Euclidean distance of z-normalized data has been shown to outperform clustering of the non-normalized counterpart, reinforcing the data preprocessing strategy adopted here (Tsumoto & Hirano, 2004). Although frequently used, and computationally efficient, Euclidean distance is not without its shortcomings. Unlike Euclidean distance, DTW is a distance measure capable of matching observations at different time points in order to achieve optimal nonlinear alignments, albeit with certain constraints (Silva *et al.*, 2018). Although computationally intensive, DTW can provide nonlinear time-scaling invariance when comparing series that are locally out of phase (“warping”) (Silva *et al.*, 2013).

The dendrogram generated by hierarchical clustering will result in a different number of clusters (k) depending on the height of the cut-point: the height of each cluster node is proportional to the value of the intergroup dissimilarity between its daughter nodes (Hastie *et al.*, 2009). We have no previous knowledge of the cut level necessary to form an ideal number of clusters, but an interpretable k can be inferred from the relative heights of the dendrogram branches and their compactness and differentiation in shape. Following initial assessment of the overall cluster dendrogram that was generated, and given that the time-series data span 19 years, we chose to analyze in detail the variability and heterogeneity of the patterns of individual growth by partitioning into $k = 20$ clusters. The R code reproducing the data preprocessing steps of scale circulus spacing reinterpolation,

z-scoring and LOESS smoothing – together with the hierarchical clustering of the processed data, the cluster dendrograms and the cluster membership heatmaps – are available at <https://bitbucket.org/arpmarquesm/scales-growth-patterns/src/master/>. Also available in this repository is a sample of the data input to the R code for the three scales. The full data necessary to reproduce the results in this paper are available upon request.

2.1.2 | Cluster description

For each cluster, a LOESS regression model was fit, based on the members of that cluster ($\alpha = 0.75$). Clusters also were characterized by the categorical variables of fish year class (*i.e.*, year of migratory return and capture) and the observed growth pattern. For the purpose of characterization, the cluster proportions for the different categories of the aforementioned variables were compared to the same proportions in the overall population, using the *catdes* function in package *FactoMineR* (Husson *et al.*, 2019). We can compare the proportion of individuals from a given year (*e.g.*, 1993) within a cluster (N_{cl1993}/N_{cl}) to the proportion of the individuals from 1993 in the population (N_{1993}/N):

$$N_{cl1993}/N_{cl} = N_{1993}/N$$

Under the null hypothesis of independence, the proportions are equal. The number of individuals N_{cl1993} follows the hypergeometric $H(N, N_{1993}, N_{cl})$. From this, the probability of equal or larger values of N_{cl1993} can be calculated, and also for the remaining years and for other categorical variables, and sorted by ascending order of P value. A corresponding v -test value can be determined from the quantile of the normal distribution which is associated with that P value. For a P value $< 5\%$, one category is significantly linked to another category, with positive or negative v -test outcomes indicating that the category is over- or under-expressed, respectively (Lê *et al.*, 2008). Here, we assessed significant over- or under-representation of growth pattern categories across the 20 clusters, as well as amongst the 19 years.

2.1.3 | Clustering as a classification tool

Prior knowledge of scale characteristics (*e.g.*, growth pattern), through visual identification of a circulus pattern for the individual fish, requires expert knowledge and is time-consuming. The hierarchical clustering algorithms explored here can therefore serve as a classification tool to identify clusters of scales that share similarities in their circulus spacing characteristics. The predominant class in each of the 20 clusters, grouped according to their similarities in shape, may agree with the visual, subjective, allocation of growth pattern for each scale. Given that the growth pattern variable comprised many possible sequences, this ultimately was split to distinguish the 10 predominant observed patterns (F, FC, FCF, FCS, FS, SF, SFC, SFCF, SFCS, SFS) of

moderate to high frequency ($n = 48$ to 563 fish; total = 1670 fish), with pooling of the 39 other patterns ($n = 234$ fish) of low frequency. For 43 fish the spacing of circuli was too heterogeneous to permit their visual classification: these were categorized as Variable (V), seven of which showed a clear Check sequence. All V scales were pooled with the "Other" category.

The utility of the cluster algorithm was assessed partly on the ability to visually predict the most frequent growth pattern category, or categories, within each cluster. The visual classification of the cluster growth pattern was compared to (a) the most frequent category or categories within each cluster and (b) the most significant categories characterizing the cluster obtained from the previous methodology, as described by Husson *et al.* (2019).

2.2 | SST anomalies and correlation analyses

Sea surface temperature (SST) anomalies for the Norwegian Sea were derived from the NOAA OISSTv2 $1 \times 1^\circ\text{C}$ gridded data set (www.cdc.noaa.gov). We took the monthly averaged data for each gridbox and removed the average seasonal cycle by applying the 1971–2000 climatology of Reynolds *et al.* (2002), thereby generating monthly anomalies for each grid box. We then calculated the average monthly anomaly for two spatially weighted kernels, of standard deviation 250 and 500 km, centred on 67.5°N , 4.5°E in the Norwegian Sea (Boehme *et al.*, 2014; Todd *et al.*, 2008). That region of the Norwegian Sea is known to embrace the ocean area to which Scottish 1SW salmon migrate (Todd *et al.*, 2008).

To interrogate possible time-series changes in the observed frequencies of scale growth pattern, we calculated correlations between the proportions of specific scale patterns over time in relation to the monthly SST kernel anomalies during the period March–September of each year. The salmon data for correlation analysis were lagged by -1 year to match their post-smolt growth season to the monthly SST data. The correlation analyses focused on the annual changes in frequency of (a) the Fast (F) growth pattern, (b) the Slow-Fast (SF) pattern, and (c) the pooled annual data for all growth patterns that showed one or more Check (C) sequence(s): this latter grouping included seven scales (amongst the total of 1947 fish) that were categorized as Variable (V). When summed together within years, the Fast and all Check groupings accounted for between 47% (2009, 2010) and 90% (2006) of the scales sampled in any one year, with an annual median of 79% .

River North Esk smolts emigrate to sea between early April and early June, and the post-smolt ocean growth season extends to November/December, at which time individuals variously show the commencement of the formation of the winter annulus on the scale (Todd *et al.*, 2014). Because both the SST and salmon time-series data show varying degrees of autocorrelation this had to be accounted for prior to the assessment of correlation significance. We did so by applying the method of Pyper and Peterman (1998) in calculating the required reductions of the degrees of freedom (from a maximum of 17) that were applied to the correlation coefficients. For the Fast data,

the applied degrees of freedom ranged from 17 down to 9 , whilst for the All Check data these ranged from 17 to 13 .

3 | RESULTS

3.1 | Hierarchical clustering and cluster silhouettes

The combination of hierarchical clustering linkage functions (Simple, Average, Complete and Ward's) and the two distance measures (Euclidean and DTW) generated a total of eight strategies. The selected linkage methods, used in combination with either the DTW or Euclidean distance measures, performed very similarly in terms of the cluster variable characterization. To ease interpretability, the outcome of the strategy that afforded less computational expense for hierarchical clustering – Ward-linkage and the Euclidean distance measure – is reported here in detail.

Figure 1 illustrates the hierarchical clustering results for $k = 20$ clusters. This value of k provided relatively high intracluster similarity, as indicated by the compactness and distinction of the cluster silhouettes (Figure 1b), whilst maintaining an informative level of user interpretability. The overall structure here indicated two main branches that derive from five sub-branches. Sub-branch A comprised clusters 1–5, with cluster 1 including only 19 scales and clusters 2–5 a further 305 scales. Cluster 1 was distinct among the overall 20 groupings in showing a markedly symmetrical bimodality to the LOESS fit. Clusters 2–5 showed varying silhouettes, albeit with the consistent feature of negative skew of the LOESS fits. By contrast, the six clusters of the largest grouping, sub-branch B ($n = 678$ scales), were each characterized by positive skew and a relatively early peak in their maximum intercirculus spacing. Sub-branch C (clusters 12–15; $n = 387$) showed a consistent pattern of an early minor peak in spacing, followed by a larger peak and a steep decline in spacing towards the ends of their sequences. Clusters 16 and 17 (sub-branch D) included 194 scales, and both their silhouettes indicated a late increase in spacing rising to a minor peak immediately prior to the winter annulus. The final sub-branch E (clusters 18–20; $n = 364$) showed lesser positive skew than did sub-branch B, but a rather progressive decline in intercirculus spacing to the commencement of the winter annulus.

3.2 | Hierarchical clustering: growth patterns amongst clusters

Figures 2 and 3 summarize the under/over-representation of the more common growth patterns and years, respectively, amongst the $k = 20$ clusters. The SF growth pattern was over-represented for four of the five clusters of sub-branch A, in association with general under-representation of patterns showing an initial Fast (F) sequence (Figure 2). Sub-branch B revealed an essentially inverse structure to sub-branch A, with sporadic over-representation of patterns commencing with a Fast sequence and under-representation of those with an initial Slow sequence. Sub-branches C and D were heterogeneous

Dendrogram Sub-branch																				Cluster	
A					B						C				D		E			Pattern	<i>n</i>
1	2	3	4	5	6	7	8	9	10	11	12	13	14	15	16	17	18	19	20		
			-			+				-		+		-	+	-	+	-	+	F	563
	-	-				-				+		+	+	+						FC	282
	-	-	-	-	+		+	+			-			+						FCF	277
	-	-	-				-		+			-							+	FCS	197
	-	-	-					+	+										+	FS	150
	-					+			+			-								Other	101
	+	+	+	+	-	-			-					-					-	SF	101
			+			-	-	-	-		+	+	+		-					SFC	90
						-													+	SFCF	78
				+		-													+	SFCS	60
				+		-														SFS	48

FIGURE 2 Tabulation of significant under- and over-representation of the 10 most frequent growth pattern categories (and “Others”) for *Salmo salar* scales amongst the 20 dendrogram clusters. Proportions of growth pattern frequency were compared to the overall population proportion of scales for $k = 20$ with Ward linkage, and clustering of the z-scored and interpolated data. Light shading (-) indicates significant under-representation and dark shading (+) indicates over-representation. Sample sizes (*n*) for each growth pattern across the time-series are shown

Dendrogram Sub-branch																				Cluster	
A					B						C				D		E			Year	<i>n</i>
1	2	3	4	5	6	7	8	9	10	11	12	13	14	15	16	17	18	19	20		
19	82	83	59	81	151	76	65	190	36	160	103	126	53	105	79	115	143	120	101		
			-				-										+		+		1993
		-	-		+		-			+						-					1994
						-				+							-				1995
				+													-				1996
	-	-	-			+		+			-				+						1997
						+															1998
					+																1999
			-		-							+		+							2000
							+	+											+		2001
	-	-	-		+			+		+	-							+			2002
					-	-			+		+	-		+					+		2003
					+						-							+			2004
			-						+								-				2005
							+					+	-								2006
			-									+			+						2007
					-	-							+				+	-			2008
	+	+	+	+	-	-	-	-						-			+	-	-		2009
+	+	+			-	-					+						-	-	-		2010
	+	+	+	+	-	-	-	-									+	-	-		2011

FIGURE 3 Tabulation of significant under- and over-representation of the 20 dendrogram clusters amongst years of capture of return adult *Salmo salar*. Details as for Figure 2

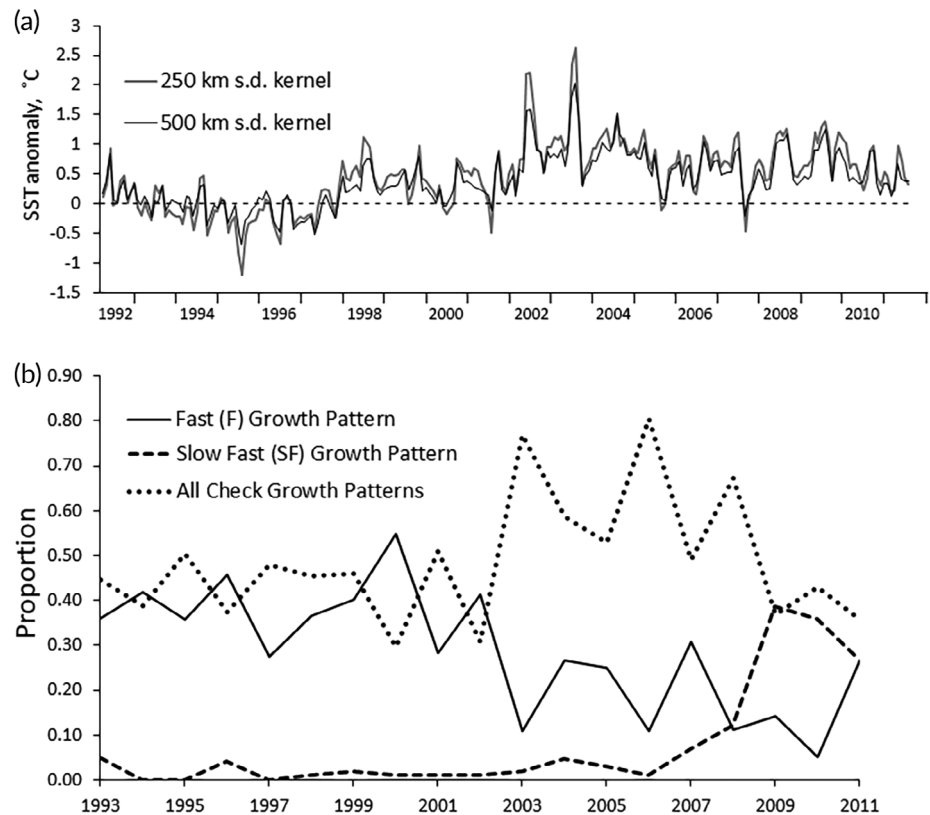
in including over-representation both of initially Fast and initially Slow sequences. For sub-branch E, the SF growth pattern was consistently under-represented and initially Fast sequences were sporadically over-represented.

3.3 | Hierarchical clustering: clusters and growth patterns among years

With respect to evidence of temporal structure along the time-series (Figure 3), the most striking feature across all sub-branches was the apparent transition in overall structure that was discernible from capture years 2007–08 (i.e., post-smolt growth seasons 2006–07)

onward. The final years of the series were characterized by widespread under-representation of sub-branches B and E, and marked over-representation of sub-branch A. The later years therefore were characterized by growth patterns including an initial Slow sequence, and - in the case of sub-branch A - especially by the SF growth pattern (Figure 2). With specific regard to those selected patterns including a Check (C) sequence in Figure 2, all five sub-branches showed evidence of their over-representation, with sub-branches B and C particularly over-represented for FC and FCF but with sub-branch C over-represented also by SFC. For cluster 17 (sub-branch D), its over-representation between capture years 2008 and 2011 (Figure 3) was linked also to over-representation of the SFCF and SFCS growth patterns (Figure 2).

FIGURE 4 Time-series changes in ocean surface temperature and *Salmo salar* scale growth pattern. (a) Changes in monthly SST anomaly for the 250 and 500 km standard deviation spatially weighted kernels in the Norwegian Sea (April 1992 – March 2011). (b) Changes in frequency (proportion within years) of selected growth patterns. The three selected pattern groupings illustrate fish showing persistent Fast growth (F) throughout the post-smolt growth season, Slow growth followed by Fast growth (SF), and all patterns pooled that displayed one or more growth Checks. The growth pattern data for each capture year (b) are aligned with the SST anomaly in April of the previous year (a), coinciding with the commencement of annual smolt emigration



3.4 | Time-series changes in growth pattern and SST anomaly

Time-series changes in the frequencies of three illustrative groupings of growth pattern are shown in Figure 4b, in association with the changes in SST anomaly for the 250 and 500 km spatially weighted kernels in the Norwegian Sea (Figure 4a). The selected groupings included those scales showing (a) consistently Fast growth (F) ($n = 563$), (b) initially Slow growth followed by Fast growth (SF) ($n = 150$) and (c) all scales pooled that included one or more Check sequences (All Check) ($n = 946$).

The SF growth pattern was consistently rare across the majority of years, but showed a marked increase in frequency over the final 5 years. By contrast, both the F and All Check groupings were consistently of moderate frequency across the early years but showed a striking – and largely inverse – divergence from 2003 onwards. The correlations between the monthly SST anomalies and frequency of the F and All Check groupings are shown in Figure 5. The two SST kernels revealed the same overall pattern of correlation, indicating that the influence of SST change during the early months of the post-smolt growth period was both pervasive and widespread throughout the Norwegian Sea. The outcome of the SST correlation analyses indicated that the effects of recent anomalous warming of the surface waters in the Norwegian Sea were manifest from the time of the earliest smolt emigrations from the River North Esk in early April, and persisted until August of the post-smolt marine growth season.

3.5 | Time-series changes in size of salmon by midwinter

Figure 4b shows that there was (a) a decrease in the frequency of fish showing consistently Fast growth throughout the post-smolt period, (b) an increase in the frequency of the SF growth pattern and (c) an increase in the frequency of growth patterns including one or more Check sequences. Furthermore, these time-series changes in circulus pattern were linked significantly to contemporaneous and anomalous warming of the Norwegian Sea (Figure 5). As shown in Figure 6, one proximate consequence of these changes is manifest in the back-calculated mean length of fish at the midpoint of the winter annulus, following the completion of the post-smolt growth season. This showed a marked and significant decrease across the final six capture years of the time series.

4 | DISCUSSION

Despite the curtailment or closure of many high seas and coastal targeted salmon fisheries, the abundance of Atlantic salmon throughout the North Atlantic region has declined markedly over the past four decades (e.g., Chaput, 2012; Gregory *et al.*, 2018; ICES, 2018). With specific reference to Scotland, a recent analysis of the ICES Working Group on North Atlantic Salmon (ICES, 2018) reported that the general decline in prefishery abundance of maturing salmon was forecast to continue. These declines likely reflect falling survivorship at sea

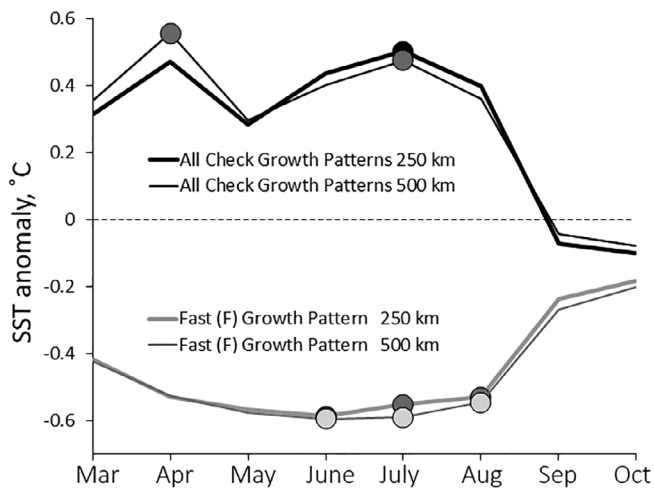


FIGURE 5 Monthly correlations between the SST anomalies throughout the post-smolt *Salmo salar* growth period and annual frequency of the Fast (F) and All Check growth patterns. The salmon data were lagged by -1 year to match the annual post-smolt growth seasons to the SST anomalies. Significant correlations ($P < 0.05$; following adjustment of d.f. to allow for autocorrelation) are shown by the filled circles

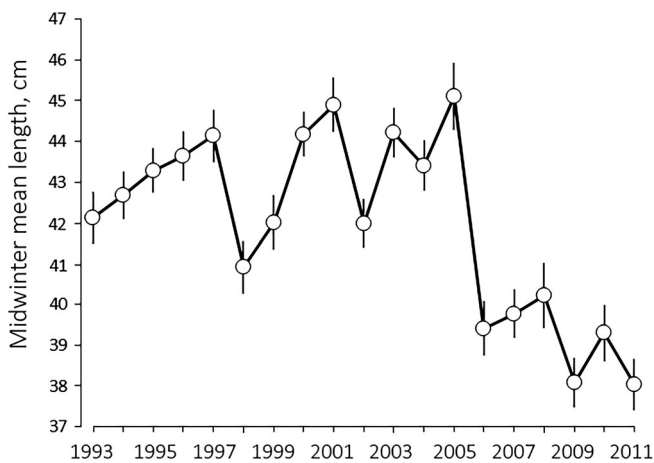


FIGURE 6 Back-calculated mean body length ($\pm 95\%$ confidence interval) of *Salmo salar* at the midpoint of the winter annulus, following the conclusion of the post-smolt growth period

(Olmos *et al.*, 2019), but it is important to note that run-timing of returning 1SW adults in Scotland has shown progressive delays since the turn of the millennium (Todd *et al.*, 2012) and that marine growth amongst European stocks also has been compromised in recent decades (Bacon *et al.*, 2009; Bal *et al.*, 2017; Jonsson *et al.*, 2016; Todd *et al.*, 2008).

The perception is that these changes in growth performance and phenology are not a direct physiological response of salmon to a warming ocean climate, but are indirectly driven by ocean warming and manifest as changes in the availability of epipelagic prey to

salmon at sea (*e.g.*, Beaugrand & Reid, 2012; Jonsson *et al.*, 2016; Nicola *et al.*, 2018; Piou & Prévost, 2013; Todd *et al.*, 2008). Any such changes in prey availability to salmon may be pervasive throughout the duration of the marine migration, or perhaps they may present as marked seasonality and/or spatial heterogeneity. Hence, it can be argued that detailed appraisals of the variation in individual growth performance from analysis of scale intercirculus spacings, their temporal patterns and linkage to physical aspects of the exploited environment ought to prove additionally informative in furthering our understanding of factors underlying the recent decline in survivorship and growth of salmon at sea. Nonetheless, it has to be emphasized that data such as the present – obtained from time-series monitoring of home water commercial catches for an identifiable river stock – are derivable only for those fish that successfully survived the marine migration to return as adults. We presently have no information for River North Esk fish that failed to survive.

The LOESS fits for all $k = 20$ dendrogram clusters (Figure 1b) showed a variable, but qualitatively consistent, pattern of circulus spacing increasing to a maximum and then decreasing towards the commencement of the winter annulus. This is not dissimilar to the observations by Peyronnet *et al.* (2015) for 1SW adults returning to the Burrishoole catchment (western Ireland) between 1961 and 1999. They noted intercirculus spacings generally to increase to a FSM and to decline thereafter toward the winter annulus. However, it is notable that whilst Peyronnet *et al.* (2015) recorded a general pattern of the FSM occurring within the first half of the sequence of post-smolt circuli, here (Figure 1b) the location of the peak or peaks of circulus spacing were temporally very variable within the interpolated circulus sequence. It is important to note, however, that data such as the present – and for Peyronnet *et al.* (2015) – do not include allowance for variation in the timing of smolt emigration of the sampled individuals. Estimates of the rate of deposition of the earliest post-smolt circuli for wild salmon typically indicate an interval of approximately 6 days (Jensen *et al.*, 2012; Todd *et al.*, 2014). Accordingly, a smolt entering the sea in early June would probably deposit up to 10 fewer circuli over the post-smolt marine growth period compared to a smolt emigrating in early April. Should those two fish encounter identical marine growth conditions (and hence pattern of marine circulus spacing) throughout the post-smolt period, then the June emigrant will show an earlier FSM because it was “missing” the early marine circuli deposited by the April emigrant. It is notable that, for example, all nine clusters in sub-branches B and E (Figure 1b) are characterized by the peak occurring within the first half of the sequence. Conversely, for sub-branch C (clusters 7–11) the peak was intermediate, whilst for clusters 2–5 of sub-branch A the peak occurred during the second half of the circulus sequence.

The contrasts between the present results and those of Peyronnet *et al.* (2015) probably are largely explicable by consideration of over-representation of our visually allocated growth patterns across the dendrogram (Figures 2, 3). For clusters 2–5 of sub-branch A we recorded a consistent over-representation of the SF pattern, manifest as a strongly negative skew of the cluster silhouettes. By contrast, sub-branch E (clusters 18–20) showed significant over-

representation of growth patterns either with a persistent Fast sequence (F) or an initial Fast sequence (FS, FCS), and hence markedly positive skew. From consideration both of Figures 2 and 3 it is clear that over the final 4–5 years of the time-series (adult capture years 2007–2011) the incidence of the SF growth pattern was significantly under-represented in sub-branches B and E (cf. clusters 2–5 of sub-branch A). These results, in addition to the marked increase over time in the incidence of the SF pattern and Checks (Figure 4b), indicate a widespread and perhaps fundamental time-series shift or deterioration of qualitative and/or quantitative aspects of the post-smolt growth environment for salmon during the earliest phase of their marine migration. Figures 4 and 5 illustrate also an apparent linkage between the recent and persistent positive SST anomalies and these shifts in post-smolt salmon growth pattern. Although the present data do not include allowance for possible changes in timing of smolt emigration from the River North Esk, the detrimental effects of recent anomalous warming of the Norwegian Sea on post-smolt growth are apparent from the marked decline, over the final 6 years of the time-series, in estimated mean body length attained by midwinter (Figure 6).

Preliminary evidence of significant correlations between recent SST warming in the Norwegian Sea and declines in the condition factor of Scottish adult 1SW salmon was provided by Todd *et al.* (2008). They showed that the somatic condition factor (weight at given length) of the return adults was driven by the SST anomaly in January, at the beginning of the second (pre-adult) growth season prior to migratory return. From the present analyses (Figure 5) it is clear that positive SST anomalies contemporaneous with the commencement of smolt emigration (early April), and throughout the early months of the post-smolt growth season (June–August), also have exerted a significant positive effect on the incidence and frequency of growth Checks. The converse outcome – of a reduction in the frequency of the F growth pattern – also is apparent. But it is important to emphasize here that these two groupings together account for a high proportion (48–91%) of the scales within any one year. Hence, a marked decrease in one would lead to an increase in the other. Nonetheless, and in addition to the initial finding of Todd *et al.* (2008) – that the post-winter SST anomaly correlated with final adult condition factor – we clearly show here that SST anomalies during the first (post-smolt) growth season have exerted additional major influences on body length growth up to the one ocean midwinter.

Given our decision to assess the dendrogram for $k = 20$ clusters, it was inevitable that high incidences of some or all of the growth patterns would characterize multiple clusters. Thus, the fact that Figures 2 and 3 do reveal a high degree of interpretable structure, and that all 10 of the common growth patterns were significantly over- and/or under-represented in one or more clusters and sub-branches (Figure 2), provides clear support for our subjective visual distinction of the various growth patterns. Especially acute, and temporally extended, periods of poor growth opportunities during the post-smolt growth season are most likely to be manifest as growth Checks in the circulus pattern of given individual fish. Amongst the present dendrogram clusters (Figure 1a), of the 17 occurrences of significant over-

representation of patterns including a Check sequence (Figure 2), nine were for those including an intermediate Check (e.g., FCS or SFCS) and eight were for terminal Check sequences (e.g., FC or SFC) immediately prior to the winter annulus. In first reporting the incidence of marked growth “checks” on scales from Scottish salmon, MacLean *et al.* (2000) noted most to occur within the second half of the circulus sequence comprising the post-smolt growth season. This was observed also for the present data (unpublished observation), leading to positive skew of the LOESS fits for given clusters. Consideration of the methodology of Todd *et al.* (2014) for estimating calendar dates of circulus deposition would indicate these Checks typically to pertain to the months of September–November prior to the formation of the winter annulus. A Check sequence of three to six circuli during the second half of the post-smolt growth period would indicate a period of markedly reduced growth persisting for perhaps up to 3–6 weeks (Todd *et al.*, 2014). Such a protracted growth hiatus implies a major constraint on foraging of salmon at sea. In this respect, we believe that the classification and categorization of visibly obvious scale growth Checks and dating of scale circulus deposition might be especially informative in identifying periods – or distinct geographic areas within the ocean migratory trajectory – that currently are especially critical to salmon at sea.

Irrespective of the subjective allocation of growth patterns, our application of hierarchical clustering has permitted the resolving of clear structure within the available time-series of circulus spacing patterns. Given the widespread occurrence of marked growth hiatuses (“false checks”; Ottaway & Simkiss, 1977) during the active growth season of teleost fish species, we would argue that the present methods offer a broadly applicable tool for analyzing environmental influences on fish growth. Within the present salmon time-series, the most marked temporal shift in post-smolt growth performance in the marine environment was for the latter four or five adult return years, and much of the variation within and between the identified dendrogram clusters was indeed explicable by the visually allocated pattern. The indications are, therefore, of a major shift in the typical post-smolt growth trajectory which occurred amongst fish returning to Scotland in the later years of the time-series. That timing matches similar contemporaneous declines in marine growth of adult 1SW salmon from southern Norwegian rivers (Jonsson *et al.*, 2016). Our data show that the incidence of a late hiatus (= Check) has increased, whilst more fish also encountered poor growth (= initial Slow) throughout the first few weeks or months of the marine migration (Figure 5). We therefore believe that this analytical approach can readily offer an effective synthesis of variation in the growth environment experienced both by species of Pacific and Atlantic salmon at sea, and perhaps provide informative linkage to size-related mortality during the marine migration (e.g., Friedland *et al.*, 2000, 2009; Peyronnet *et al.*, 2015).

ACKNOWLEDGEMENTS

Helen Kenn assisted extensively with image analysis and data collation, and we thank Tania Mendo for comments on an early draft of the manuscript. The initial stages of this work were supported by

funding for C.D.T. from the CERC Aquatic Epidemiology Visiting Scientist initiative at University of Prince Edward Island. Support for A.R.M. during this study was provided by the Canada Excellence Research Chair in Aquatic Epidemiology.

AUTHOR CONTRIBUTIONS

C.D.T. and N.N.H. developed the initial ideas and the acquisition of scale data. L.B. provided the analysis of the oceanographic data. C.W.R. and A.R.M. undertook the cluster analyses and C.D.T., N.N.H., L.B., C.W.R. and A.R.M. all contributed to the writing and preparation of the manuscript.

ORCID

Christopher D. Todd  <https://orcid.org/0000-0002-9690-2839>

REFERENCES

- Bacon, P. J., Palmer, S. C. F., MacLean, J. C., Smith, G. W., Whyte, B. D. M., Gurney, W. S. C., & Youngson, A. F. (2009). Empirical analyses of the length, weight, and condition of adult Atlantic salmon on return to the Scottish coast between 1963 and 2006. *ICES Journal of Marine Science*, *66*, 844–859. <https://doi.org/10.1093/icesjms/fsp096>.
- Bal, G., Montorio, L., Rivot, E., Prévost, E., Baglinière, J.-L., & Nevoux, M. (2017). Evidence for long-term change in length, mass and migration phenology of anadromous spawners in French Atlantic salmon *Salmo salar*: changing *S. salar* size and phenology. *Journal of Fish Biology*, *90*, 2375–2393. <https://doi.org/10.1111/jfb.13314>.
- Beaugrand, G., & Reid, P. C. (2012). Relationships between North Atlantic salmon, plankton, and hydrodynamic change in the Northeast Atlantic. *ICES Journal of Marine Science*, *69*, 1549–1562. <https://doi.org/10.1093/icesjms/fss153>.
- Bilton, H. T., & Ricker, W. E. (1965). Supplementary checks on the scales of pink salmon (*Oncorhynchus gorboscha*) and chum salmon (*O. keta*). *Journal of the Fisheries Research Board of Canada*, *22*, 1477–1489. <https://doi.org/10.1139/f65-127>.
- Bilton, H. T., & Robins, G. L. (1971). Effects of feeding level on circulus formation on scales of young sockeye salmon (*Oncorhynchus nerka*). *Journal of the Fishery Research Board of Canada*, *28*, 861–868. <https://doi.org/10.1139/f71-126>.
- Boehme, L., Lonergan, M., & Todd, C. D. (2014). Comparison of gridded sea surface temperature datasets for marine ecosystem studies. *Marine Ecology Progress Series*, *516*, 7–22. <https://doi.org/10.3354/meps11023>.
- Britton, J. R. (2010). Scale circuli patterns differentiate between hatchery-reared and wild *Rutilus rutilus* during evaluation of fish stocking. *Journal of Fish Biology*, *77*, 2454–2459. <https://doi.org/10.1111/j.1095-8649.2010.02800.x>.
- Casselman, J. M. (1987). Determination of age and growth. In A. H. Weatherley & H. S. Gill (Eds.), *The biology of fish growth* (pp. 209–242). London: Academic Press.
- Chaput, G. (2012). Overview of the status of Atlantic salmon (*Salmo salar*) in the North Atlantic and trends in marine mortality. *ICES Journal of Marine Science*, *69*, 1538–1548. <https://doi.org/10.1093/icesjms/fss013>.
- DeVries, D. R., & Frie, R. V. (1996). Determination of age and growth. In B. R. Murphy & D. W. Willis (Eds.), *Fisheries techniques* (2nd ed., pp. 483–512). Bethesda, MD: American Fisheries Society.
- Friedland, K. D., Reddin, D. G., & Kocik, J. F. (1993). Marine survival of North American and European Atlantic salmon: effects of growth and environment. *ICES Journal of Marine Science*, *50*, 481–492. <https://doi.org/10.1006/jmsc.1993.1051>.
- Friedland, K. D., & Haas, R. E. (1996). Marine post-smolt growth and age at maturity of Atlantic salmon. *Journal of Fish Biology*, *48*, 1–15. <https://doi.org/10.1111/j.1095-8649.1996.tb01414.x>.
- Friedland, K. D., Hansen, L. P., Dunkley, D. A., & MacLean, J. C. (2000). Linkage between ocean climate, post-smolt growth, and survival of Atlantic salmon (*Salmo salar* L.) in the North Sea area. *ICES Journal of Marine Science*, *57*, 419–429. <https://doi.org/10.1006/jmsc.1999.0639>.
- Friedland, K. D., Clarke, L. M., Dutil, J.-P., & Salminen, M. (2006). The relationship between smolt and postsmolt growth for Atlantic salmon (*Salmo salar*) in the Gulf of St Lawrence. *Fishery Bulletin*, *104*, 149–155.
- Friedland, K. D., MacLean, J. C., Hansen, L. P., Peyronnet, A. J., Karlsson, L., Reddin, D. G., ... McCarthy, J. L. (2009). The recruitment of Atlantic salmon in Europe. *ICES Journal of Marine Science*, *66*, 289–304. <https://doi.org/10.1093/icesjms/fsn210>.
- Fisher, J. P., & Percy, W. G. (1990). Spacing of scale circuli versus growth rate in young coho salmon. *Fishery Bulletin*, *88*, 637–643.
- Fisher, J. P., & Percy, W. G. (2005). Seasonal changes in growth of coho salmon (*Oncorhynchus kisutch*) off Oregon and Washington and concurrent changes in the spacing of scale circuli. *Fishery Bulletin*, *103*, 34–51.
- Fukuwaka, M. A., & Kaeriyama, M. (1997). Scale analyses to estimate somatic growth in sockeye salmon, *Oncorhynchus nerka*. *Canadian Journal of Fisheries and Aquatic Sciences*, *54*, 631–636. <https://doi.org/10.1139/f96-307>.
- Gregory, S. D., Armstrong, J. D., & Britton, J. R. (2018). Is bigger really better? Towards improved models for testing how Atlantic salmon smolt size affects marine survival. *Journal of Fish Biology*, *92*, 579–592. <https://doi.org/10.1111/jfb.13550>.
- Hanson, N. N., Smith, G. W., Middlemas, S. J., & Todd, C. D. (2019). Precision and accuracy of Dahl-Lea back-calculated smolt lengths from adult scales of Atlantic salmon (*Salmo salar* L.). *Journal of Fish Biology*, *94*, 183–186. <https://doi.org/10.1111/jfb.13863>.
- Haraldstad, T., Haugen, T. O., Borgström, R., & Jonsson, B. (2016). Increased precision of growth data gained by reading multiple scales from each individual of Atlantic salmon (*Salmo salar*). *Fauna Norvegica*, *36*, 1–7. <https://doi.org/10.5324/fn.v36i0.1954>.
- Hastie, T., Tibshirani, R., & Friedman, J. (2009). *The elements of statistical learning: data mining, inference and prediction* (2nd ed.). Berlin: Springer.
- Hogan, F., & Friedland, K. D. (2010). Retrospective growth analysis of Atlantic salmon *Salmo salar* and implications for abundance trends. *Journal of Fish Biology*, *76*, 2502–2520. <https://doi.org/10.1111/j.1095-8649.2010.02650.x>.
- Husson, F., Josse, J., Lê, S., & Mazet, J. (2019). FactoMineR: Multivariate Exploratory Data Analysis and Data Mining. R package version 1.41.
- Ibañez, A. L., Britton, J. R., & Cowx, I. G. (2008). Relationship between scale growth checks, circuli formation rate and somatic growth in *Rutilus rutilus* (L.) a fish-farm-reared cyprinid. *Journal of Fish Biology*, *72*, 1023–1034. <https://doi.org/10.1111/j.1095-8649.2007.01781.x>.
- ICES (2018). Report of the Working Group on North Atlantic Salmon (WGNAS), 4–13 April 2018, Woods Hole, MA, USA. ICES CM 2018/ACOM:21. p. 386. http://ices.dk/sites/pub/Publication%20Reports/Expert%20Group%20Report/acom/2018/WGNAS/wgnas_2018.pdf
- Jensen, A. J., ÓMaoláidigh, N., Thomas, K., Einarsson, S. M., Haugland, M., Erkinaro, J., ... Østborg, G. M. (2012). Age and fine-scale marine growth of Atlantic salmon post-smolts in the Northeast Atlantic. *ICES Journal of Marine Science*, *69*, 1668–1677. <https://doi.org/10.1093/icesjms/fss086>.
- Jonsson, B., Jonsson, N., & Albretsen, J. (2016). Environmental change influences the life history of salmon *Salmo salar* in the North Atlantic Ocean. *Journal of Fish Biology*, *88*, 618–637. <https://doi.org/10.1111/jfb.12854>.
- Keogh, E., & Kasetty, S. (2003). On the need for time series data mining benchmarks: a survey and empirical demonstration. *Data Mining and Knowledge Discovery*, *7*, 349–371. <https://doi.org/10.1023/A:1024988512476>.

- MacLean, J. C., Smith, G. W., & Whyte, B. D. M. (2000). Description of marine growth checks observed on the scales of salmon returning to Scottish home waters in 1997. In D. Mills (Ed.), *The Ocean Life of Atlantic salmon. Environmental and Biological Factors Influencing Survival* (pp. 37–48). Oxford, UK: Fishing News Books; Blackwell Science.
- McCarthy, J. L., Friedland, K. D., & Hansen, L. P. (2008). Monthly indices of the post-smolt growth of Atlantic salmon from the Drammen River, Norway. *Journal of Fish Biology*, 72, 1572–1588. <https://doi.org/10.1111/j.1095-8649.2008.01820.x>.
- Nicola, G. G., Elvira, B., Jonsson, B., Ayllón, D., & Almodóvar, A. (2018). Local and global climatic drivers of Atlantic salmon decline in southern Europe. *Fisheries Research*, 198, 78–85. <https://doi.org/10.1016/j.fishres.2017.10.012>.
- Olmos, M., Massiot-Granier, F., Prévost, E., Chaput, G., Bradbury, I. R., Nevoux, M., & Rivot, E. (2019). Evidence for spatial coherence in time trends of marine life history traits of Atlantic salmon in the North Atlantic. *Fisheries Research*, 20, 322–342. <https://doi.org/10.1111/faf.12345>.
- Ottaway, E. M., & Simkiss, K. (1977). A method for assessing factors influencing 'false check' formation in fish scales. *Journal of Fish Biology*, 11, 681–687. <https://doi.org/10.1111/j.1095-8649.1977.tb05724.x>.
- Peyronnet, A., Friedland, K. D., ÓMaoléidigh, N., Manning, M., & Poole, W. R. (2015). Links between patterns of marine growth and survival of Atlantic salmon *Salmo salar*, L. *Journal of Fish Biology*, 71, 684–700. <https://doi.org/10.1111/j.1095-8649.2007.01538.x>.
- Piou, C., & Prévost, E. (2013). Contrasting effects of climate change in continental vs. oceanic environments on population persistence and microevolution of Atlantic salmon. *Global Change Biology*, 19, 711–723. <https://doi.org/10.1111/gcb.12085>.
- Pyper, B. J., & Peterman, R. M. (1998). Comparison of methods to account for autocorrelation in correlation analyses of fish data. *Canadian Journal of Fisheries and Aquatic Sciences*, 55, 2127–2140.
- R Core Team. (2018). *R: A language and environment for statistical computing*. Vienna: R Foundation for Statistical Computing.
- Ratanamahatana, C. A., & Keogh, E. (2004). Everything you know about Dynamic Time Warping is wrong. In *KDD-2004. Proceedings of third workshop on mining temporal and sequential data* (pp. 22–25). New York, NY: ACM.
- Reddin, D. G., & Friedland, K. D. (1999). A history of identification to continent of origin of Atlantic salmon (*Salmo salar* L.) at west Greenland, 1969–1997. *Fisheries Research*, 43, 221–235. [https://doi.org/10.1016/S0165-7836\(99\)00074-0](https://doi.org/10.1016/S0165-7836(99)00074-0).
- Reynolds, R. W., Rayner, N. A., Smith, T. M., Stokes, D. C., & Wang, W. Q. (2002). An improved *in situ* and satellite SST analysis for climate. *Journal of Climate*, 15, 1609–1625. [https://doi.org/10.1175/1520-0442\(2002\)015<1609:AIISAS>2.0.CO;2](https://doi.org/10.1175/1520-0442(2002)015<1609:AIISAS>2.0.CO;2).
- Sardá-Espinosa, A. (2017). Comparing time-series clustering algorithms in R using the Dtwclust package, pp. 1–45. Vienna: R Development Core Team. <https://cran.r-project.org/web/packages/dtwclust/vignettes/dtwclust.pdf>.
- Sardá-Espinosa, A. (2018). Dtwclust: time series clustering along with optimizations for the Dynamic Time Warping distance. R package version 5.5.1. <https://CRAN.R-project.org/package=dtwclust>.
- Shearer, W. M. (1992). *Atlantic salmon scale reading guidelines*. ICES Cooperative Research Report, No. 188 (p. 46). Copenhagen: International Council for the Exploration of the Sea.
- Silva, D.F., de Souza, V.M.A. & Batista, G.E.A.P.A. (2013). Time series classification using compression distance of recurrence plots. 13th International Conference on Data Mining, Dallas, TX, pp. 687–696. <https://doi.org/10.1109/ICDM.2013.128>.
- Silva, D. F., Giusti, R., Keogh, E., & Batista, G. (2018). Speeding up similarity search under Dynamic Time Warping by pruning unpromising alignments. *Data Mining and Knowledge Discovery*, 32, 988–1016. <https://doi.org/10.1007/s10618-018-0557-y>.
- Tattam, I. A., Whitesel, T. A., & Pan, Y. D. (2003). Scale pattern analysis of selected scale characteristics and the first annulus for distinguishing wild and hatchery steelhead in the Hood River, Oregon. *North American Journal of Fisheries Management*, 23, 856–868. <https://doi.org/10.1577/M02-027>.
- Thomas, K., Hansen, T., Brophy, D., Maoiléidigh, N. Ó., & Fjelldal, P. G. (2019). Experimental investigation of the effects of temperature and feeding regime on scale growth in Atlantic salmon *Salmo salar* post-smolts. *Journal of Fish Biology*, 94, 896–908. <https://doi.org/10.1111/jfb.13971>.
- Todd, C. D., Hughes, S. L., Marshall, C. T., MacLean, J. C., Lonergan, M. E., & Biuw, E. M. (2008). Detrimental effects of recent ocean warming on growth condition of Atlantic salmon. *Global Change Biology*, 14, 958–970. <https://doi.org/10.1111/j.1365-2486.2007.01522.x>.
- Todd, C. D., Friedland, K. D., MacLean, J. C., Whyte, B. D., Russell, I. C., Lonergan, M. E., & Morrissey, M. B. (2012). Phenological and phenotypic changes in Atlantic salmon populations in response to a changing climate. *ICES Journal of Marine Science*, 69, 1686–1698. <https://doi.org/10.1093/icesjms/fss151>.
- Todd, C. D., Whyte, B. D. M., MacLean, J. C., Revie, C. W., & Hanson, N. N. (2014). A simple method of dating marine growth circuli on scales of wild one sea-winter and two sea-winter Atlantic salmon (*Salmo salar*). *Canadian Journal of Fisheries and Aquatic Sciences*, 71, 645–655. <https://doi.org/10.1139/cjfas-2013-0359>.
- Tsumoto, S., & Hirano, S. (2004). A comparative study of clustering methods for long time-series medical databases. In V. Torra & Y. Narukawa (Eds.), *Modeling decisions for artificial intelligence* (pp. 260–272). Berlin: Springer.
- Weyl, O. L. F., & Booth, A. J. (1999). On the life history of a cyprinid fish, *Labeo cylindricus*. *Environmental Biology of Fishes*, 55, 215–225. <https://doi.org/10.1023/A:1007543319416>.

How to cite this article: Todd CD, Hanson NN, Boehme L, Revie CW, Marques AR. Variation in the post-smolt growth pattern of wild one sea-winter salmon (*Salmo salar* L.), and its linkage to surface warming in the eastern North Atlantic Ocean. *J Fish Biol.* 2020;1–11. <https://doi.org/10.1111/jfb.14552>